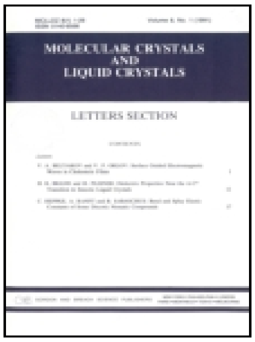

Molecular Crystals and Liquid Crystals

ISSN: 1542-1406 (Print) 1563-5287 (Online) Journal homepage: http://www.tandfonline.com/loi/gmcl20

Dielectric Properties of 4-Cyano-4'-pentylbiphenyl (5CB): 4-[4-(S)-2-Methylbutoxybenzoyloxy]benzoic Acid (BAC) Composite

N. Yilmaz Canli, Z. Güven Özdemir, M. Okutan, D. Güzeller, H. Ocak & B. Bilgin Eran

To cite this article: N. Yilmaz Canli, Z. Güven Özdemir, M. Okutan, D. Güzeller, H. Ocak & B. Bilgin Eran (2015) Dielectric Properties of 4-Cyano-4'-pentylbiphenyl (5CB): 4-[4-(S)-2-Methylbutoxybenzoyloxy]benzoic Acid (BAC) Composite, Molecular Crystals and Liquid Crystals, 623:1, 17-30, DOI: 10.1080/15421406.2014.990753

To link to this article: http://dx.doi.org/10.1080/15421406.2014.990753

Mol. Cryst. Liq. Cryst., Vol. 623: pp. 17–30, 2015
Copyright © Taylor & Francis Group, LLC
ISSN: 1542-1406 print/1563-5287 online
DOI: 10.1080/15421406.2014.990753

Dielectric Properties of 4-Cyano-4′-pentylbiphenyl (5CB): 4-[4-(S)-2-Methylbutoxybenzoyloxy]benzoic Acid (BAC) Composite

N. YİLMAZ CANLİ,[1,*] Z. GÜVEN ÖZDEMİR,[1] M. OKUTAN,[1]
D. GÜZELLER,[2] H. OCAK,[2] AND B. BİLGİN ERAN[2]

[1]Yildiz Technical University, Department of Physics, Istanbul, Turkey
[2]Yildiz Technical University, Department of Chemistry, Istanbul, Turkey

Dielectric relaxation dynamics properties of ***5CB*** *(4-cyano-4′-pentylbiphenyl) and* ***BAC****(4-[4-(S)-2-methylbutoxybenzoyloxy]benzoic acid) have been investigated. In this respect, dielectric properties of* ***5CB*** *plus* ***(1%)BAC*** *have been compared with* ***5CB****. The polarizing microscopy results show that* ***BAC*** *and* ***5CB*** *exhibit enantiotropic N* mesophase and N mesophase, respectively. The real (ε ′) and imaginary components (ε′′) of dielectric constant have been calculated by capacitance method. The dielectric relaxation mechanisms of liquid crystals have been analyzed by Cole-Cole plots and the Debye distribution parameters (α) have been calculated. It has been also determined that adding* ***BAC*** *to* ***5CB*** *increases the voltage dependent dielectric strength.*

Keywords 4-[4-(S)-2-Methylbutoxybenzoyloxy]benzoic acid; 4-cyano-4′-pentylbiphenyl; absorption coefficient; dielectric strength; liquid crystal; relaxation mechanism

1. Introduction

Liquid crystals (LCs) represent a special state of soft matter with properties of liquids and solid state crystals. LCs have restricted or even absent long-range positional order, but there is a long-range orientational correlation between the molecules. There are two broad groups of LCs: thermotropic and lyotropic. Thermotropic LCs exhibit a phase transition into the LC phase as temperature is changed, whereas lyotropic LCs exhibit phase transitions as a function of mesogen concentration in a solvent as well as temperature. Depending on compound, LC materials have rod-like elongated, banana-shaped, or disk-like molecules [1,2].

In a nematic LCs, molecules have long-range correlation of the orientations of their long axes but not of their positions. In a smectic material, molecules stay within certain equidistant planes, as a result smectic molecules display both long-range positional and orientational order. If molecules' planes are normal to the director, the crystalline structure is defined as uniaxial (Smectic A), otherwise it is biaxial (Smectic C). Other type of LCs

---

[*] Address correspondence to N. Yilmaz Canli, Yildiz Technical University, Department of Physics, 34210 Istanbul, Turkey. E-mail: niyilmaz@yahoo.com

Color versions of one or more of the figures in the article can be found online at www.tandfonline.com/gmcl.

is chiral, in such material molecules show a twist of the long axis and director is normal to the twist axis. If molecules have no long-range positional order, LC material is called chiral nematic or cholesteric. Chiral LC with the long-range positional order is called chiral smectic.

In this study, the chiral nematic LC (N*) has been investigated. In the simplest case of a uniaxial nematic LC (NLC), the molecules are predominantly aligned along a single direction called a director. The director can be realigned by electric and magnetic fields that results change of the optical properties of sample. The orientational dynamics of director under the influence of applied electric field is a fundamental physical phenomenon that locates at the heart of modern display technologies [3]. With the development of liquid crystal displays, creation of new LC materials with high dielectric anisotropy and low viscosity have attracted a great deal of attention [4]. The dielectric anisotropy of NLCs plays important role for display applications [5].

Determination of the physical properties of liquid crystalline compounds strongly depends on the information about molecular shape and intermolecular interactions. A small change in molecular structure can result in a dramatic change in the corresponding liquid crystal properties. The physical and optical properties of liquid crystals can be developed by doping of different liquid crystals and hence improvement of electronic and optical properties of new liquid crystal composite can be achieved.

Liquid crystal mixtures with positive dielectric anisotropy are used for the most active matrix displays for the development of image quality of LCDs [6]. Dielectric spectroscopy method is used to obtain a reliable information about the molecular and dielectric properties of nematic liquid crystals.

The main goal of dielectric studies has been focused on a relationship between dielectric constant and molecular properties of liquid crystals [7]. The dielectric properties of liquid crystals play an important role in determining the electro-optical response of liquid crystal devices. As is known, the real and imaginary part of dielectric function, dielectric loss, conductivity, and capacitance are crucial parameters for deciding the suitable material for technological applications. For example, relatively higher dielectric constants are used in microelectronic devices such as capacitors, memory devices etc.

4-cyano-4′-pentylbiphenyl (**5CB**) is one of the best-known liquid crystalline substances. **5CB**, as well as other members of the *n*CB homologous series, is important from the point of view of applications due to the possession of a strong dipole moment, good chemical stability, and a convenient temperature range of the nematic phase [8]. From this point of view, this work is devoted to enhance the dielectric properties **5CB** by adding 1% (w/w) 4-[4-(S)-2-Methylbutoxybenzoyloxy]benzoic acid **(BAC)** chiral nematic (N*) liquid crystal composite.

2. Theoretical

2.1. Capacitance Method for Calculation of Dielectric Parameters

The theoretical background of dielectric calculations is given as follows. When an alternative voltage $V = V_o \exp(i\omega t)$ is applied to the air filled capacitor, the charging current, $(I)_{\mathrm{air}}$ is given by

$$(I)_{\mathrm{air}} = i\omega C_{\mathrm{air}} V \tag{1}$$

Air filled capacitance, C_{air} is defined as the ratio of charge on the parallel plates and voltage applied. When an alternative voltage $V = V_o \exp(i\omega t)$ is applied to the liquid crystal filled capacitor, the total current (I_{total}) is written as the sum of charging current $(I)_{\mathrm{LC}} = \mathrm{i}\omega C_{\mathrm{LC}} V$ and $I = GV = (1/R)V$ which is due to conductance (G) through the dielectric.

$$I_{\mathrm{total}} = (I)_{\mathrm{LC}} + I = i\omega C_{\mathrm{LC}} V + GV \tag{2}$$

where the capacitance of liquid crystal material is defined as

$$C_{\mathrm{LC}} = \varepsilon_r C_{\mathrm{air}} \tag{3}$$

Dielectric constant ε_r is defined as $\varepsilon / \varepsilon_0$. By using Eq. (3) in Eq. (2), one can write the total current in terms of the real and imaginary components of permittivity:

$$I_{\mathrm{total}} = i\omega(\varepsilon_r' - i\varepsilon_r'')\, C_{\mathrm{air}}\, V \tag{4}$$

ε_r is the complex dielectric constant ($\varepsilon_r = \varepsilon_r{}' \text{-} i\varepsilon_r{}''$). Conductance, G is given by Eq. (5).

$$G = \omega\varepsilon_r'' C_{\mathrm{air}} = (\omega\varepsilon_r''\, \varepsilon_0)\,(A/d) = \omega\, \varepsilon''(A/d) \tag{5}$$

In Eq. (5), ε'' denotes the imaginary part of dielectric constant. A and d represent the area of parallel plates and the distance between the plates, respectively.

The relation between the real and imaginary component of dielectric constant is given by the concept of loss factor (i.e., dielectric loss or dissipation factor), tanδ [9].

$$\tan\delta = \varepsilon''/\varepsilon' \tag{6}$$

2.2. Determination of Dielectric Relaxation Mechanism by Cole-Cole Plots

Dielectric relaxation behavior is originally derived from Debye relaxation model. In this model, real and imaginary parts of dielectric constant can be represented by Fig. 1.

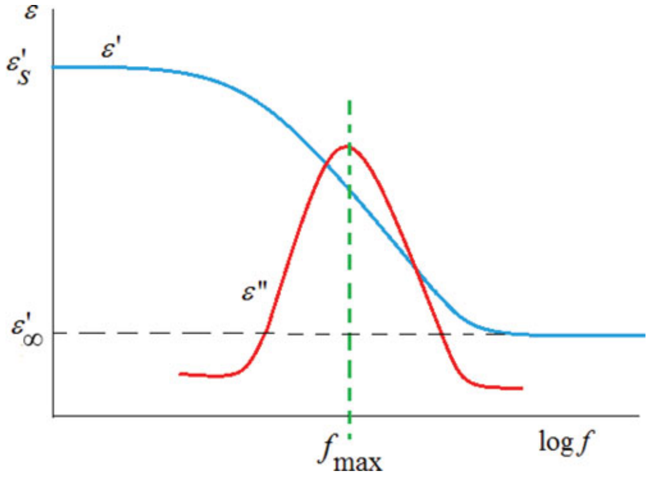

Figure 1. Debye dielectric dispersion curve [10].

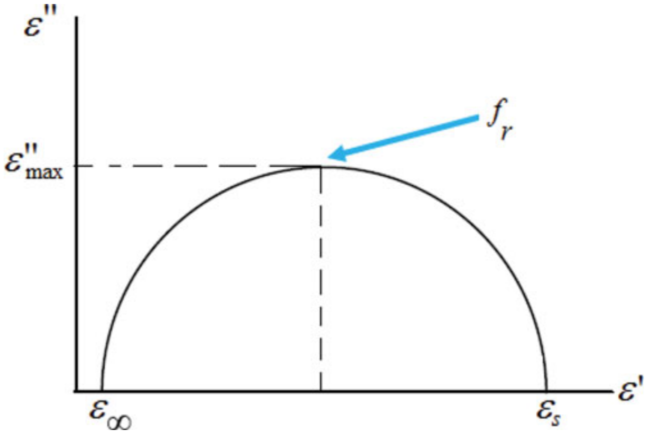

Figure 2. Debye type relationship between dielectric constant and dielectric loss by Cole-Cole plots [11].

The complex dielectric dispersion curves are described by the Cole-Cole relation [11–13],

$$\varepsilon^*(\omega) = \varepsilon_\infty + \frac{\varepsilon_s - \varepsilon_\infty}{1 + (i\omega\tau)^{1-\alpha}} \tag{7}$$

where $\varepsilon^*(\omega)$ is the complex dielectric constant, ε_s is the limiting low-frequency dielectric constant, ε_∞ is the limiting high-frequency dielectric constant, τ is the average relaxation time, ω is the average angular frequency, and α is the distribution parameter (absorption coefficient). Eq. (7) determines the relaxation time distribution that manifests itself in the shape of the Cole-Cole diagrams [11]. The α parameter takes values between 0 and 1 [14].

In the pure Debye model ($\alpha = 0$), the dipoles are assumed to be noninteracting with each other. The plots indicate semi-circles centered on the ε'-axis as shown in Fig. 2. The complex dielectric dispersion relation for polar dielectrics at the low and high-frequency regions can be written by

$$\begin{aligned}\varepsilon'(\omega) = \varepsilon'_I(\omega) + \varepsilon'_{II}(\omega) &= \left[\varepsilon_{1\infty} + (\varepsilon_{1s} - \varepsilon_{1\infty})\frac{1 + (\omega\tau_1)^{1-\alpha_1}\sin\frac{1}{2}\alpha_1\pi}{1 + 2(\omega\tau_1)^{1-\alpha_1}\sin\frac{1}{2}\alpha_1\pi + (\omega\tau_1)^{2(1-\alpha_1)}}\right] \\ &+ \left[\varepsilon_{2\infty} + (\varepsilon_{2s} - \varepsilon_{2\infty})\frac{1 + (\omega\tau_2)^{1-\alpha_2}\sin\frac{1}{2}\alpha_2\pi}{1 + 2(\omega\tau_2)^{1-\alpha_2}\sin\frac{1}{2}\alpha_2\pi + (\omega\tau_2)^{2(1-\alpha_2)}}\right]\end{aligned} \tag{8}$$

where $\varepsilon'_I(\omega)$ and $\varepsilon'_{II}(\omega)$ are the real parts for the low and high-frequency regions, respectively.

The maximum loss occurs at the midpoint between the two dielectric values of ε_s and ε_∞ that coincides with $\varepsilon''_{\max}$. Frequency at which dielectric loss is maximum, is defined as a relaxation frequency f_r of the orientational polarization. The frequency, where the semi-circle crossed with ordinate axis, corresponds to the minimum dielectric loss.

Table 1. Phase transition temperatures T (°C) of **BAC**; Cr: crystalline, N*: chiral nematic, and Iso: isotropic phase

Liquid crystal	Phase transition temperatures T (°C)
BAC	Cr 168 N* 184 Iso

3. Experimental

3.1. Synthesis of Liquid Crystals

The preparation procedure, spectroscopic, and mesomorphic data for 4-[4-(S)-2-methylbutoxybenzoyloxy]benzoic acid (**BAC**) were given in Refs. [15–18]. Transition temperatures were measured using a Linkam THMS 600 hot stage and a Linkam TMS 93 temperature control unit in conjunction with a Leitz Laborlux 12 Pol polarizing microscope (Table 1). The chemical structures of the **5CB** and **BAC** have been shown in Fig. 3.

3.2. Preparation of Liquid Crystal Cells

Empty cells have been prepared by indium-tin-oxide (ITO) coated glass plates purchased by Instec Colorada Inc. (Fig. 4a) The thickness of the empty cells was set as $d = 9 \pm 0.1\ \mu$m by Mylar spacer. We have prepared cells with planar orientation which was provided by a rubbed layer of polyimide. Before filling the cell with **5CB** and **5CB+(1%)BAC**, the capacitance of the empty cell, C_{air} has been measured by HP 4192A Impedance Analyzer.

The ITO cells have been filled with the **5CB** and **5CB+(1%)BAC** by capillary action (Fig. 4b). The schematic representations of the cells have been given in Fig. 5. R_{ITO} denotes

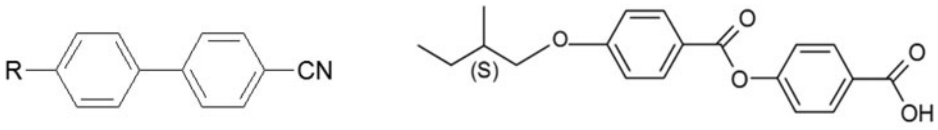

a) 5CB: R = C_5H_{11}; Cr 25 N 34 Iso

b) BAC: Cr 168 N* 184 Iso

Figure 3. The chemical structures and phase transition temperatures of **(a) 5CB** (4-cyano-4′-pentylbiphenyl) and **(b) BAC** (4-[4-(S)-2-methylbutoxybenzoyloxy]benzoic acid).

(a) **(b)**

Figure 4. **(a)** The structure and photography of empty LC cell **(b)** Filling LC cell with capillary effect.

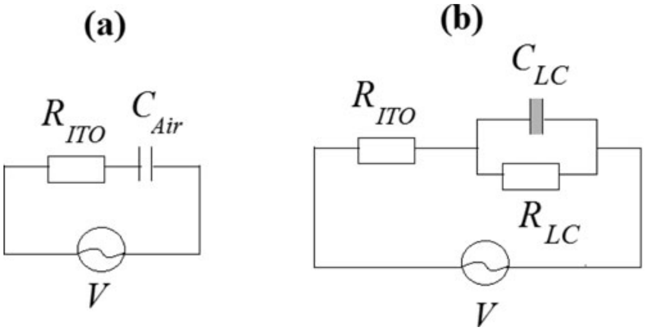

Figure 5. The schematic representation of ac voltage applied equivalent circuit of **(a)** an empty cell **(b)** the cell filled with LC.

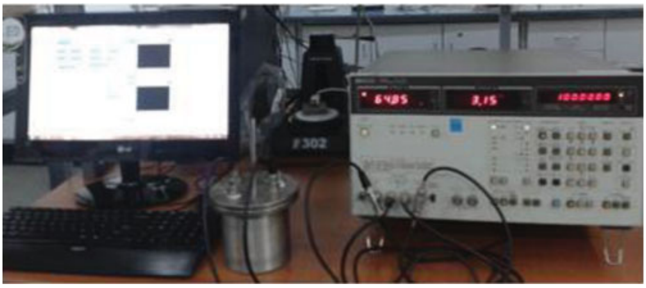

Figure 6. The photography of experimental set-up.

the resistance of *ITO* electrodes, C_{air} represents the capacitance of the air inside the empty cell. C_{LC} and R_{LC} are also the capacitance and resistance of the LC, respectively.

3.3. Experimental Set-up

The dielectric parameters of **5CB** and **5CB+(1%)BAC** have been calculated by the capacitance method via HP 4192A LF Impedance Analyzer within the frequency range of 5 Hz—13 MHz. The LC cells were screened any electric field effects by Faraday cage. The photography of experimental system has been given in Fig. 6.

4. Results and Discussions

4.1. Liquid Crystalline Properties of the Liquid Crystal Material

(4-[4-(S)-2-Methylbutoxybenzoyloxy]benzoic acid) (**BAC**) exhibits thermotropic enantiotropic mesophase. Polarizing microscope photograph of **BAC** shows Chiral Nematic (N*) mesophase (Fig. 7). The transition temperatures for the **BAC** have been given in Table 1.

4.2 Dielectric Properties of the Liquid Crystals

The dielectric spectra of **5CB**, and **5CB+(1%)BAC** liquid crystals have been determined within the frequency range of 5 Hz–13 MHz for the voltage interval of 0—30 V. The real parts of dielectric constant of **5CB** and **5CB+(1%)BAC** have been given in Figs. 8a and 8b, respectively. As shown in Figures 8a and 8b, the real part of dielectric constants decrease while the frequency increases for all dc bias applied. On the other hand, the real part of dielectric constant has its maximum value at low frequencies. Between 400 Hz and 60 kHz, the real parts of the dielectric constant of the liquid crystals do not significantly change with frequency and then drastically decrease with increasing frequency. At lower frequencies, the real parts of the dielectric constant increase with applied voltage due to the molecular reorientation. For all dc bias applied, the high frequency values of the real components of the dielectric constant reach 0.20 and 0.18 for **5CB** and **5CB+(1%)BAC**, respectively.

As shown in Figs. 9a and 9b, the imaginary parts of dielectric constant increase while the frequency increases for all dc bias applied. The magnitude of ε'' in low frequency region is higher than that of high frequency region. Since the magnitude of ε'' is proportional to energy dissipation, it has been deduced that the system is more stable in the high frequency region.

The imaginary parts of the dielectric constants indicate two dielectric relaxation peaks ($\boldsymbol{R_1}$ and $\boldsymbol{R_2}$) that correspond to rotations of the molecules (Figs. 9a and 9b). The first peak ($\boldsymbol{R_1}$) corresponds to low frequency region and exhibits a significant frequency shift with dc bias applied. The second peak ($\boldsymbol{R_2}$) is associated with the high frequency region and it slightly shifts to low frequency region with voltage applied. In order to achieve a significant shift for relaxation frequency, the rate of the doping concentration should be increased. Both $\boldsymbol{R_1}$ and $\boldsymbol{R_2}$ relaxation processes can be related with the rotation of the molecules in LC system.

To observe the doping effect on the real and imaginary components of dielectric constant, the comparative graphics of **5CB** and **5CB+(1%)BAC** have been drawn

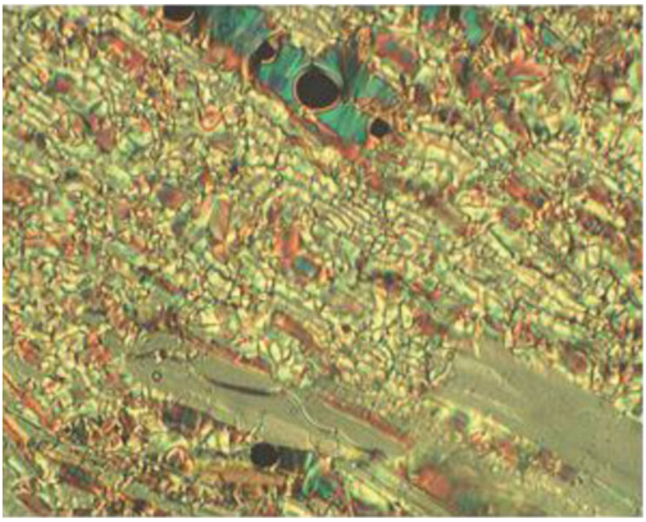

Figure 7. Polarized light optical photomicrograph of the **BAC** (Cooling at 172°C N* mesophase).

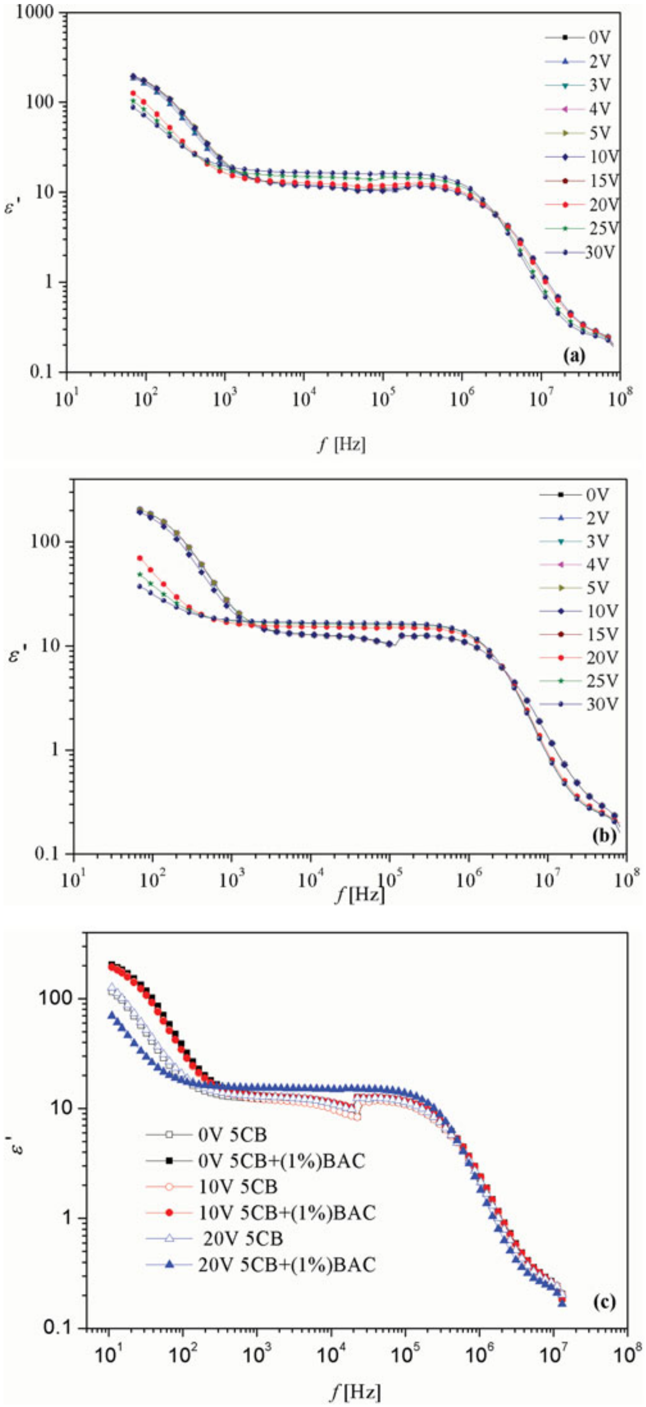

Figure 8. The real part of dielectric constant of **(a) 5CB (b) 5CB+(1%)BAC (c)** The comparative results for the real components of dielectric constant of **5CB** and **5CB+(1%)BAC** at some selected voltages.

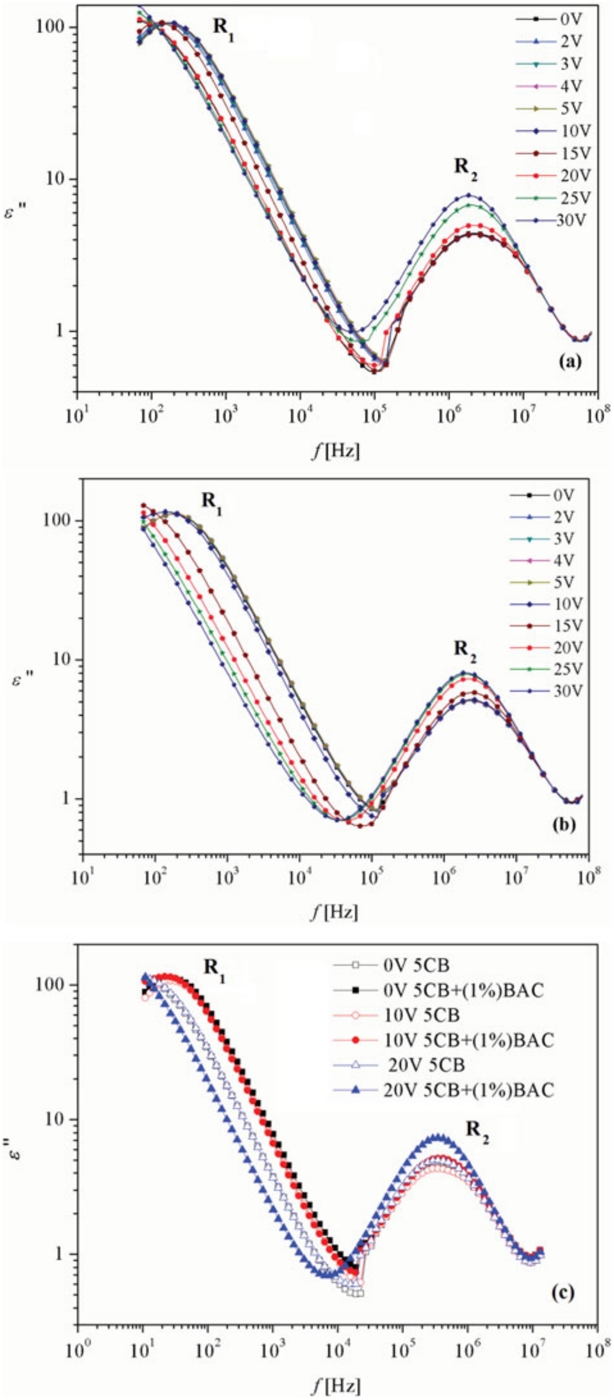

Figure 9. The imaginary part of dielectric constant of **(a) 5CB (b) 5CB+(1%)BAC (c)** The comparative results for the imaginary components of dielectric constant of **5CB** and **5CB+(1%)BAC** at some selected voltages.

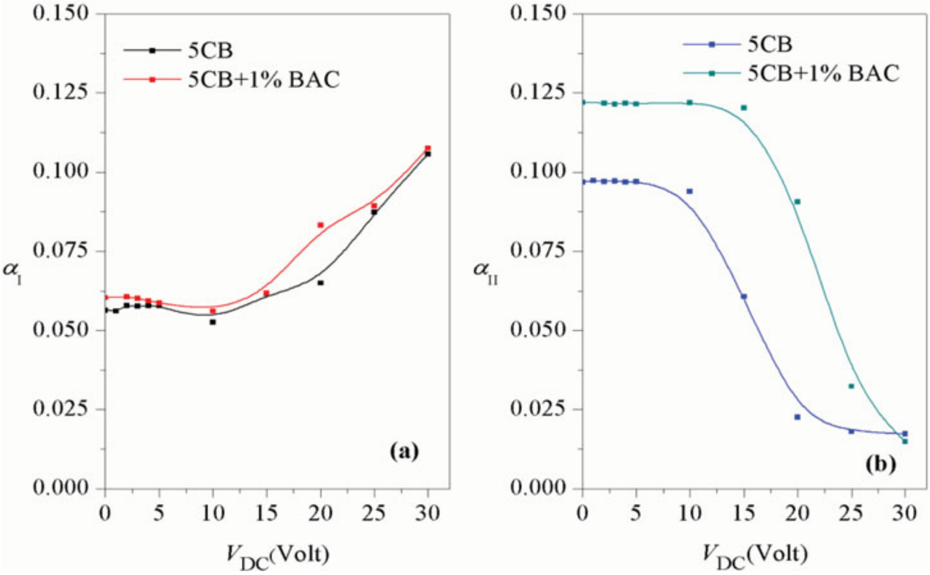

Figure 10. Bias voltage dependency of the absorption coefficient ($\alpha_{I,II}$) of **5CB** and **5CB+(1%)BAC** for the **(a)** low frequency region (I) and **(b)** high frequency region (II).

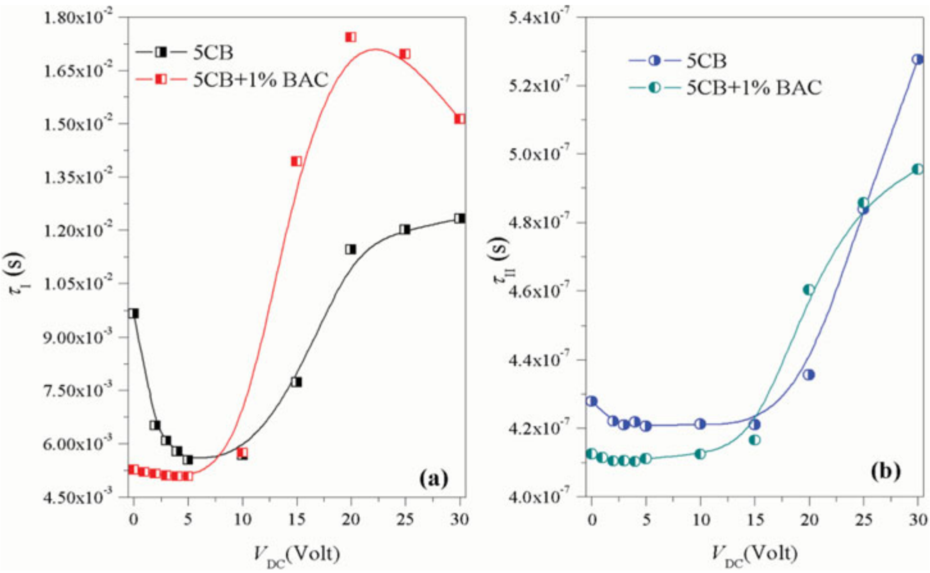

Figure 11. Bias voltage dependency of the relaxation time of **5CB** and **5CB+(1%)BAC** for the **(a)** low frequency region (I) and **(b)** high frequency region (II).

(Figs. 8c and 9c) for applied dc bias (0, 10, and 20 V). As is seen from related figures, the maximum values of ε' and ε'' also increase with (1%) **BAC** doping.

To analyze the dielectric relaxation type of **5CB** and **5CB+(1%)BAC**, the fitting functions of dielectric constant have been determined by Origin Lab. 8.5 program. We have calculated τ and α parameters from Eq. (8). The calculated absorption coefficients $\alpha_{I,\,II}$ and

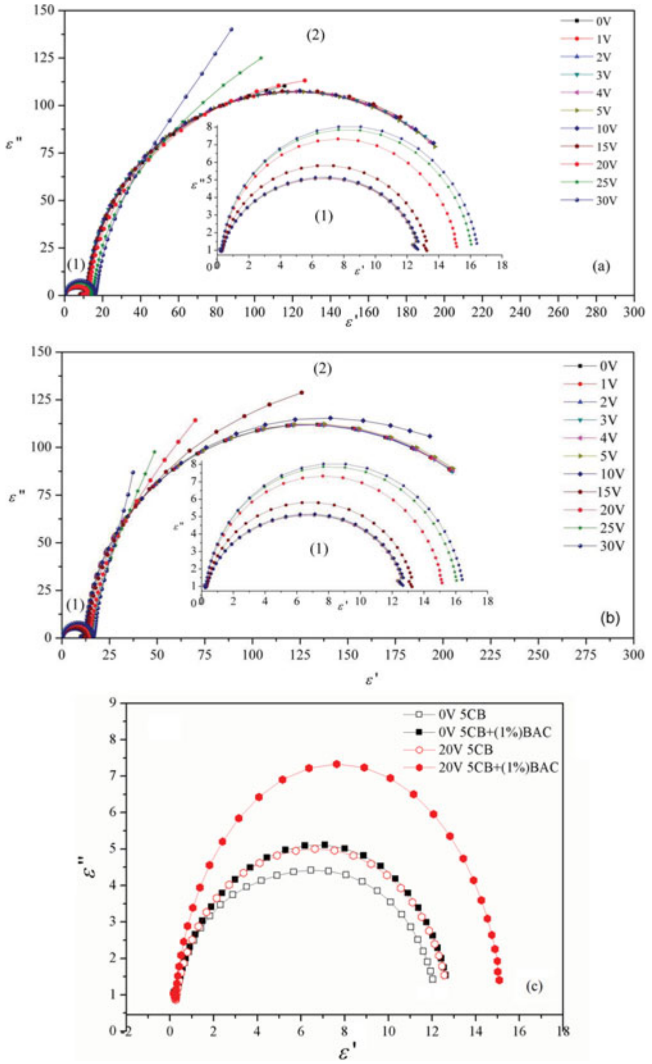

Figure 12. The Cole-Cole plots of **(a) 5CB (b) 5CB+(1%)BAC (c)** The comparative results for Cole-Cole plots at some selected voltages of **5CB** and **5CB+(1%)BAC** for the high frequency region.

relaxation times $\tau_{\mathrm{I,II}}$ for the low frequency (I) and high frequency (II) regions have been given in Figs. 10 and 11, respectively.

According to 10a and 10b, absorption coefficients increase with doping for the first (low frequency) and the second relaxation (high frequency) regions. However, adding **BAC** to **5CB** decreases α coefficient exponentially that approaches to zero which is in agreement with Debye model for high frequency region and high dc bias (Fig. 10b). Moreover, **BAC** doping to **5CB** decreases time constant for low frequency region at low dc bias interval of $0<V_{\mathrm{DC}}<8$V. **BAC** doping to **5CB** also decreases time constant for high frequency region at dc bias interval of $0<V_{\mathrm{DC}}<15$V. Since the time constant decreases with doping, the reorientation of molecules begins at low threshold voltage relative to **5CB**.

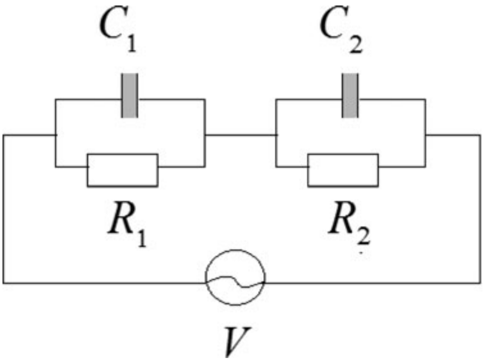

Figure 13. The equivalent circuit of Cole-Cole curves for two frequency regions.

In order to analyze dielectric relaxation mechanism of the liquid crystals, we have plotted Cole-Cole graphics for **5CB** and **5CB+(1%)BAC**. Figs. 12a, 12b and 12c show the Cole-Cole plots for different dc bias applied.

As is seen from Figs. 12a and 12b, both LCs have two different semi-circles for the high and low frequency regions which have been denoted by (1) and (2), respectively. The equivalent circuits of these semi-circles have been given in Fig. 13. The subscripts 1 and 2 for the capacitances and resistances correspond to the high and low frequency regions, respectively.

The ε_s and $\varepsilon''_{\max}$values were calculated from the Cole-Cole curves and they have been given in Table 2. The characteristics of ε_s and $\varepsilon''_{\max}$tend to increase with applied dc bias and adding different **LC** to **5CB** system.

The adding of (1%) **BAC** to **5CB** increases the dielectric strength ($\Delta\varepsilon = \varepsilon_s - \varepsilon_\infty$) with the applied dc bias (Fig. 14). The increase in the value of dielectric strength may be due to the decrease of the threshold voltage, V_{th}. Hence the reorientation of molecules in **5CB+(1%)BAC** requires less voltage than **5CB**.

Table 2. The $\varepsilon''_{\max}$, ε_s, ε_∞, and $\Delta\varepsilon$ values calculated from the Cole-Cole curves for **5CB** and **5CB+(1%)BAC**

5CB	10 V	15 V	20 V	25 V	30 V
$\varepsilon_{\max}''$	4.43	4.60	4.94	6.75	7.81
ε_s	11.86	11.89	12.54	14.69	16.26
ε_∞	0.2054	0.2052	0.2030	0.1972	0.1920
$\Delta\varepsilon$	11.654	11.684	12.337	14.492	16.068
5CB+(1%)BAC	10 V	15 V	20 V	25 V	30 V
$\varepsilon_{\max}''$	5.12	5.78	7.27	7.80	8.02
ε_s	12.68	13.36	15.22	16.16	16.58
ε_∞	0.1824	0.1781	0.1663	0.1626	0.1616
$\Delta\varepsilon$	12.497	13.181	15.053	15.997	16.418

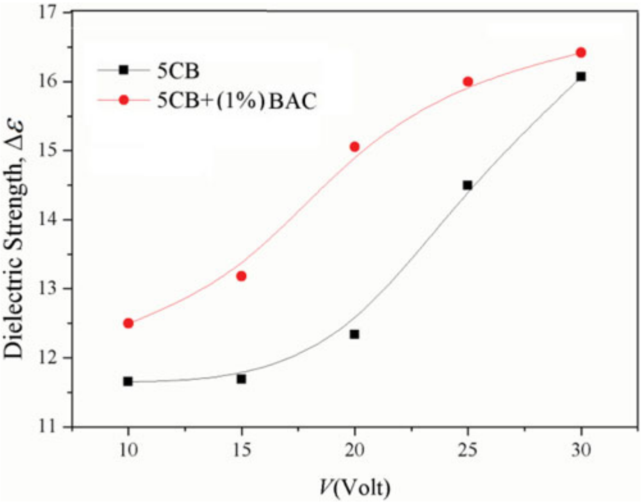

Figure 14. The variation of dielectric strength with applied dc bias for **5CB** and **5CB+(1%)BAC**.

5. Conclusions

The dielectric relaxation dynamics properties of **5CB** and **5CB+(1%)BAC** have been investigated. **BAC** and **5CB** exhibit enantiotropic N* mesophase and N mesophase, respectively.

The frequency dependent real (ε') and imaginary components (ε'') of dielectric constant have been calculated within the frequency interval of 5 Hz–13 MHz. The dielectric relaxation mechanisms of liquid crystals have been analyzed by Cole-Cole plots. It has been determined that the LC systems have two dielectric relaxation processes. The diameter of Cole-Cole plots increases with adding **BAC** and dc bias applied. As is seen from fitting results of the real part of dielectric constant, adding **BAC** to **5CB** approaches α coefficient to zero for high frequency and high dc bias. This results show that adding **BAC** to **5CB** approaches the relaxation mechanism Debye type for high frequency and high dc bias of 30 V. Moreover, it has been determined that adding (1%, w/w) **BAC** to **5CB** increases the voltage dependent dielectric strength significantly that results lower the threshold voltage. From this point of view, it has been revealed that, adding **BAC** to **5CB** speeds up the time for requiring reorientation of molecules.

Ultimately, by determining the optimum voltage value and doping concentration for the system, the desirable orientation for the devices could be achieved. Hence, this information would be helpful for the next electro-optic applications.

Acknowledgments

This work has been supported by the Scientific and Technological Research Council of Turkey (TUBITAK) with the project number: 111T102 and Yildiz Technical University Scientific Research Projects Coordination Department under Project Number: 2014-01-01-GEP05.

References

[1] De Gennes, P. G., & Prost, J. (1993). *The Physics of Liquid Crystals*, 2nd ed., Oxford University Press: Oxford.

[2] De Gennes, P. G., & Prost, J. (1997). *The Physics of Liquid Crystals*, 2nd ed., Cambridge University Press: New York.

[3] Fréedericksz, V., & Zolina, V. (1933). *Trans. Faraday Soc.*, *29*, 919–930.

[4] Chen, X., Li, H., Chen, Z., Lou, J., & Wen, J. (1999). *Liq. Crys.*, *26*, 1743–1747.

[5] Blinov, L. M., & Chigrinov, V. G. (1996). *Electrooptic Effects in Liquid Crystal Material*, Springer: New York.

[6] Yakuphanoglu, F., Okutan, M., Köysal, O., & Keum, S. R. (2008). *Dyes Pigments*, *76*, 202–206.

[7] Smyth, C. P. (1980). *Molecular Interactions*, Wiley New: York.

[8] Czub, J., Urban, S., & Würflinger, A. (2006). *Liq. Cryst. 33*, 85–89.

[9] Cavdar, Ş., Koralay, H., Tuğluoğlu, N., & Günen, A. (2005). *Supercond. Sci. Technol.*, *18*, 1204–1209.

[10] Debye, P. (1929). *Polar Molecules*, Dover Publications Chemical Catalog: New York.

[11] Cole, K. S., & Cole, R. H. (1941). *J. Chem. Phys.*, *9*, 341–352.

[12] Bunget, I., & Popescu, M. (1984). *Physics of Solid Dielectrics*, Elsevier Publishing Company: Amsterdam.

[13] Chelkowski, A. (1980). *Dielectric Physics (Studies in Physical and Theoretical Chemistry)*, Elsevier Science Ltd.: Amsterdam.

[14] Raju, G. G. (2003). *Dielectrics in Electric Fields*, Marcel Dekker: New York.

[15] Ocak, H., Bilgin Eran, B., Prehm, M., & Tschierske, C. (2013). *Soft Matter*, *9*, 4590–4597.

[16] Ocak, H., Bilgin Eran, B., Prehm, M., Schymura, S., Lagerwall, J. P. F., & Tschierske, C. (2011). *Soft Matter*, *7*, 8266–8280.

[17] Xie, M., Qin, J., Hu, Z., & Zhao, H. (1992). *Chinese Chem. Lett.*, *3*, 775–778.

[18] Jun, Q., Ming-Gui, X., Zi-Lun, H., Hua-Ming, Z., & Shi-Kui, L. (1992). *Synthetic Commun.*, *22*, 2253–2258.